CHEMELECTROCHEM

Supporting Information

Characterization of Structural and Electronic Transitions During Reduction and Oxidation of $Ru(acac)_3$ Flow Battery Electrolytes by using X-ray Absorption Spectroscopy

Jonathan F. Kucharyson, Jason R. Gaudet, Brian M. Wyvratt, and Levi T. Thompson*[a]

celc_201600360_sm_miscellaneous_information.pdf

Supporting Information

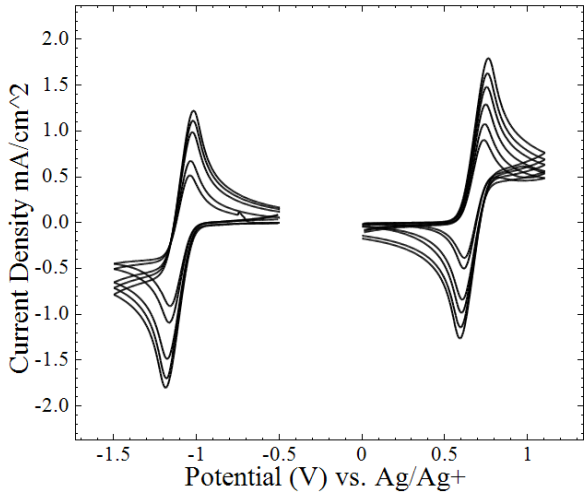

Figure S1. Cyclic Voltammograms for varying scan rates of $Ru(acac)_3$. Solutions comprised of 0.01M active species and 0.1M TBABF4 in acetonitrile.

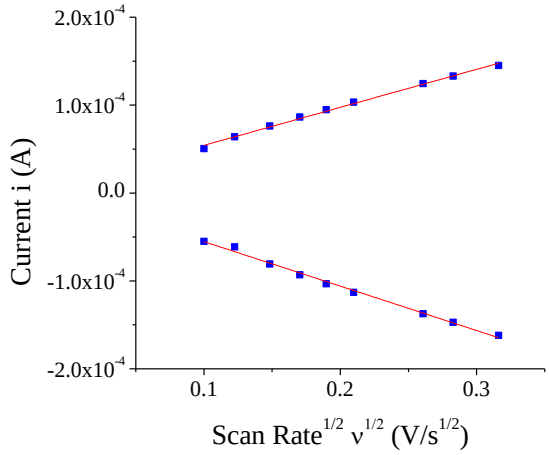

Figure S2. Current vs. Scan Rate$^{1/2}$ of negative couple of $Ru(acac)_3$. Solutions comprised of 0.01M active species and 0.1M TBABF4 in acetonitrile.

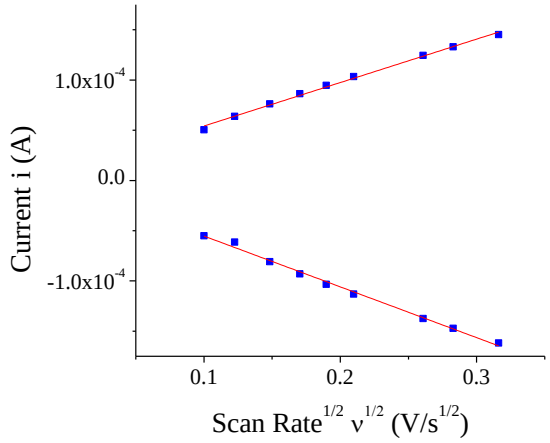

Figure S3. Current vs. Scan Rate$^{1/2}$ of positive couple of $Ru(acac)_3$. Solutions comprised of 0.01M active species and 0.1M TBABF4 in acetonitrile.

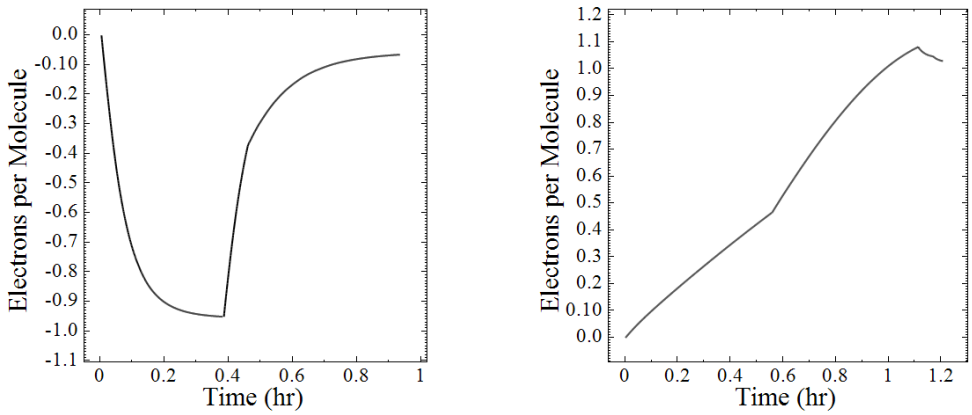

Figure S4. Electrons per molecule transferred during BE of the negative couple (left) and positive couple (right).

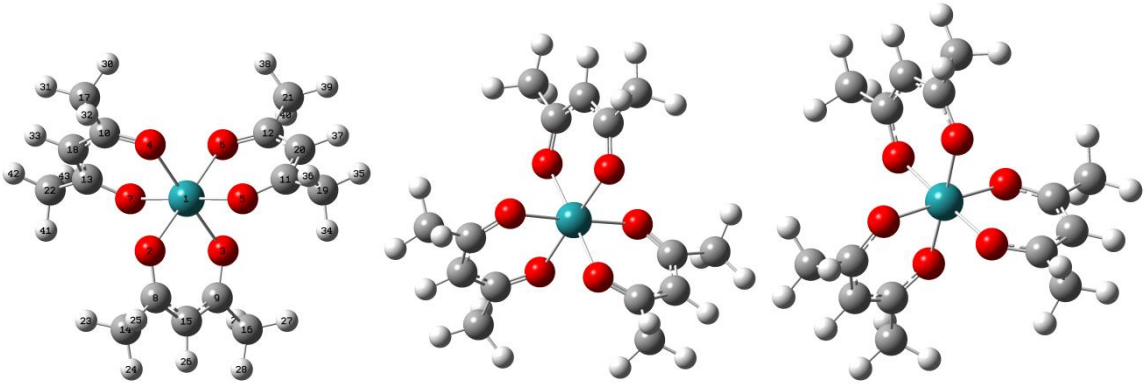

Figure S5: Gaussian optimized structures of $Ru(acac)_3$, $[Ru(acac)_3]^{+1}$ and $[Ru(acac)_3]^{-1}$.

Table S1. XYZ coordinates of Gaussian optimized $Ru(acac)_3$, $[Ru(acac)_3]^{+1}$ and $[Ru(acac)_3]^{-1}$.

Atom	$Ru(acac)_3$			$[Ru(acac)_3]^{+1}$			$[Ru(acac)_3]^{-1}$		
	X	Y	Z	X	Y	Z	X	Y	Z
Ru	0.000	0.095	0.000	0.002	0.000	0.000	0.000	-0.001	0.000
O	-0.982	-1.308	1.109	0.136	1.624	1.166	-0.747	1.521	-1.222
O	0.982	-1.308	-1.109	1.341	-0.925	1.173	0.694	-1.547	1.222
O	-0.975	1.543	1.100	-1.298	0.978	-1.171	0.994	1.372	1.224
O	1.509	0.089	1.365	1.500	0.632	-1.174	1.689	-0.117	-1.225
O	0.975	1.543	-1.100	-1.471	-0.692	1.173	-0.948	-1.406	-1.224
O	-1.509	0.089	-1.365	-0.199	-1.618	-1.168	-1.685	0.173	1.225
C	-0.825	-2.569	0.954	-0.472	2.752	1.034	-0.501	2.752	-1.032
C	0.825	-2.568	-0.954	-1.741	2.180	-1.038	1.797	-2.146	1.032
C	-2.199	1.857	0.953	-0.148	3.764	2.098	-1.146	3.689	-2.046
C	2.667	0.614	1.176	-1.373	3.055	-0.002	0.286	3.315	-0.001
C	2.198	1.857	-0.953	-1.026	-2.597	-1.034	0.963	2.626	1.032
C	-2.667	0.614	-1.176	2.621	-0.965	1.038	2.634	-0.942	-1.034
C	-1.632	-3.418	1.913	2.763	0.411	-1.040	-2.136	-1.809	-1.032
C	0.000	-3.196	0.000	-2.148	-1.780	1.040	-2.756	-0.481	1.034
C	1.632	-3.418	-1.913	-2.715	2.608	-2.102	2.107	-3.237	2.050
C	-2.738	2.814	1.995	-0.918	-3.654	-2.100	2.732	-1.903	-0.001
C	-3.046	1.414	-0.090	-1.967	-2.709	0.002	1.757	3.439	2.047
C	3.662	0.322	2.278	3.336	-1.750	2.104	3.766	-0.854	-2.051
C	3.045	1.415	0.090	3.334	-0.343	0.000	-2.628	-2.832	-2.049
C	2.738	2.814	-1.995	3.622	1.034	-2.106	-3.016	-1.411	0.002
C	-3.662	0.322	-2.278	-3.187	-2.002	2.106	-3.857	-0.202	2.052
H	-2.697	-3.185	1.801	0.935	3.929	2.130	-0.813	3.418	-3.056
H	-1.480	-4.489	1.752	-0.443	3.369	3.077	-2.235	3.562	-2.020
H	-1.353	-3.166	2.943	-0.654	4.716	1.927	-0.905	4.742	-1.863
H	0.000	-4.280	0.000	-1.818	4.042	-0.001	0.380	4.398	-0.002
H	2.697	-3.185	-1.801	-3.555	1.905	-2.134	2.125	-2.801	3.057
H	1.480	-4.488	-1.752	-2.223	2.568	-3.081	1.308	-3.989	2.037
H	1.353	-3.166	-2.943	-3.094	3.617	-1.931	3.066	-3.732	1.859
H	-2.115	3.715	2.019	0.109	-4.035	-2.137	3.623	-2.524	-0.001
H	-3.776	3.098	1.804	-1.132	-3.207	-3.078	2.805	3.114	2.038
H	-2.670	2.347	2.985	-1.605	-4.484	-1.926	1.367	3.246	3.055
H	-4.063	1.787	-0.086	-2.606	-3.584	0.001	1.717	4.516	1.851
H	3.776	-0.762	2.389	2.930	-2.768	2.145	3.365	-1.016	-3.060
H	4.641	0.769	2.083	3.149	-1.289	3.081	4.197	0.155	-2.033
H	3.274	0.706	3.229	4.412	-1.797	1.929	4.562	-1.583	-1.863
H	4.063	1.788	0.086	4.411	-0.452	0.000	-2.570	-2.401	-3.057
H	2.115	3.716	-2.019	3.430	2.112	-2.149	-1.970	-3.710	-2.034
H	3.776	3.098	-1.804	3.347	0.618	-3.083	-3.657	-3.155	-1.859
H	2.670	2.347	-2.984	4.685	0.862	-1.929	-4.000	-1.871	0.002
H	-3.776	-0.763	-2.389	-3.861	-1.139	2.148	-3.492	-0.440	3.059
H	-4.641	0.769	-2.083	-2.694	-2.075	3.083	-4.103	0.868	2.042
H	-3.275	0.706	-3.229	-3.769	-2.908	1.929	-4.768	-0.778	1.857

Table S2. Gaussian results for change of all bond lengths for $Ru(acac)_3$ during positive and negative reactions.

Atom #	Atom Type	Bond to Atom #	$Ru(acac)_3$ Bond Length [Å]	$[Ru(acac)_3]^{+1}$ Bond Length [Å]	$[Ru(acac)_3]^{-1}$ Bond Length [Å]
1	Ru	-	-	-	-
2	O	1	2.041	2.005	2.090
3	O	1	2.041	2.005	2.090
4	O	1	2.064	2.005	2.090
5	O	1	2.035	2.006	2.090
6	O	1	2.064	2.005	2.090
7	O	1	2.035	2.006	2.090
8	C	2	1.280	1.289	1.269
9	C	3	1.280	1.288	1.269
10	C	4	1.271	1.289	1.269
11	C	5	1.286	1.288	1.269
12	C	6	1.271	1.289	1.269
13	C	7	1.286	1.288	1.269
14	C	8	1.514	1.505	1.525
15	C	9	1.409	1.405	1.414
16	C	9	1.514	1.505	1.524
17	C	10	1.514	1.505	1.524
18	C	13	1.401	1.405	1.414
19	C	11	1.513	1.505	1.524
20	C	11	1.401	1.405	1.414
21	C	12	1.514	1.505	1.524
22	C	13	1.513	1.505	1.524
23	H	14	1.096	1.096	1.097
24	H	14	1.093	1.092	1.096
25	H	14	1.096	1.096	1.097
26	H	15	1.084	1.083	1.086
27	H	16	1.096	1.096	1.097
28	H	16	1.093	1.092	1.096
29	H	16	1.096	1.096	1.097
30	H	17	1.096	1.096	1.097
31	H	17	1.093	1.092	1.096
32	H	17	1.096	1.096	1.097
33	H	18	1.084	1.083	1.086
34	H	19	1.096	1.096	1.097
35	H	19	1.093	1.092	1.096
36	H	19	1.096	1.096	1.097
37	H	20	1.084	1.083	1.086
38	H	21	1.096	1.096	1.097
39	H	21	1.093	1.092	1.096
40	H	21	1.096	1.096	1.097
41	H	22	1.096	1.096	1.097
42	H	22	1.093	1.092	1.096
43	H	22	1.096	1.096	1.097

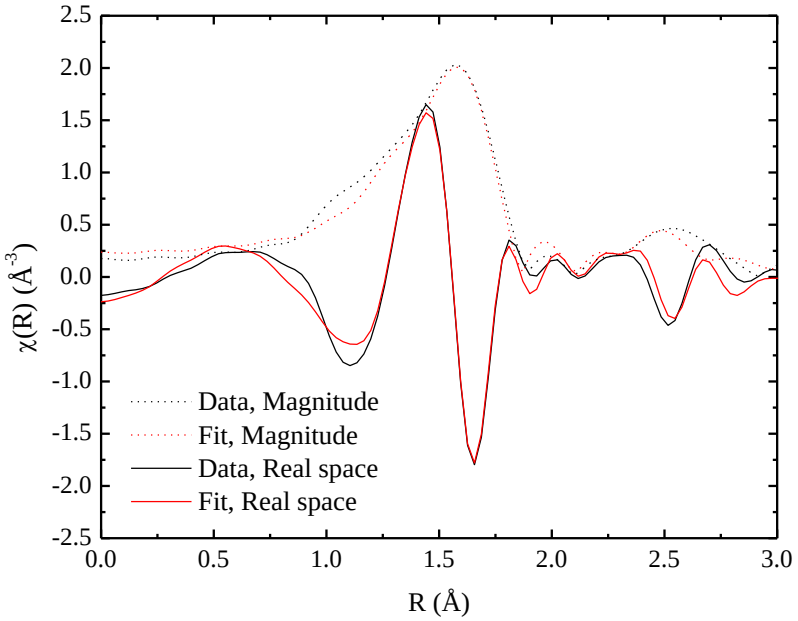

Figure S6. Example EXAFS fit of $Ru(acac)_3$ before BE expressed as the real portion (Re[χ(R)]) and magnitude (|χ(R)|) of the Fourier transform. Fitting range is 1.2<R<2.8Å.

Table S3. Full EXAFS regression parameters for $Ru(acac)_3$ during in situ negative and positive reactions.

Reaction	Direction	SOC (%)	Amplitude	ΔE_0 (eV)	σ^2 (10^3 Å^2)	R1 (Å)	R2 (Å)	R3 (Å)	O-Ru-C Angle (°)
Negative	Charging	0	1.02±0.1	1.6±1.7	2.5±0.8	2.019±0.009	2.935±0.019	3.081±0.047	14
Negative	Charging	23	1.03±0.11	2.5±1.8	2.7±0.9	2.021±0.01	2.936±0.021	3.074±0.05	14
Negative	Charging	34	1.03±0.12	3±2	2.8±1.1	2.026±0.011	2.939±0.024	3.075±0.056	14
Negative	Charging	45	0.99±0.1	2.5±1.8	2.7±1	2.034±0.01	2.943±0.022	3.086±0.052	14
Negative	Charging	55	0.99±0.1	2.7±1.7	2.8±0.9	2.041±0.01	2.946±0.021	3.093±0.05	14
Negative	Charging	71	0.99±0.1	2.7±1.7	2.8±0.9	2.048±0.009	2.95±0.021	3.098±0.05	15
Negative	Charging	77	0.99±0.11	2.9±1.8	2.8±0.9	2.051±0.01	2.951±0.021	3.101±0.054	15
Negative	Discharging	58	0.98±0.11	2.8±1.9	2.8±1	2.042±0.011	2.947±0.024	3.095±0.057	14
Negative	Discharging	45	0.98±0.11	2.3±1.8	2.7±1	2.036±0.01	2.944±0.022	3.094±0.053	15
Negative	Discharging	34	1±0.11	2.3±1.8	2.7±0.9	2.028±0.01	2.94±0.022	3.087±0.053	14
Negative	Discharging	21	1.03±0.1	2.8±1.7	2.7±0.9	2.021±0.009	2.936±0.02	3.076±0.047	14
Negative	Discharging	16	1.02±0.11	2.8±1.8	2.6±0.9	2.019±0.01	2.935±0.022	3.074±0.052	14
Positive	Charging	0	1±0.11	2.3±1.8	2.5±0.9	2.02±0.01	2.937±0.021	3.082±0.052	14
Positive	Charging	19	1.01±0.11	2.2±1.8	2.6±0.9	2.018±0.01	2.934±0.022	3.082±0.054	14
Positive	Charging	39	1±0.12	2.3±1.9	2.6±1	2.016±0.01	2.934±0.023	3.086±0.057	15
Positive	Charging	59	0.98±0.1	2.4±1.5	2.5±0.9	2.015±0.009	2.933±0.02	3.094±0.049	15
Positive	Charging	78	0.98±0.11	1.9±1.6	2.6±0.9	2.016±0.009	2.933±0.021	3.11±0.056	16
Positive	Charging	98	0.96±0.1	2±1.4	2.5±0.9	2.015±0.009	2.931±0.022	3.117±0.053	16
Positive	Charging	118	0.96±0.11	1.9±1.5	2.6±1	2.013±0.009	2.929±0.024	3.125±0.059	16

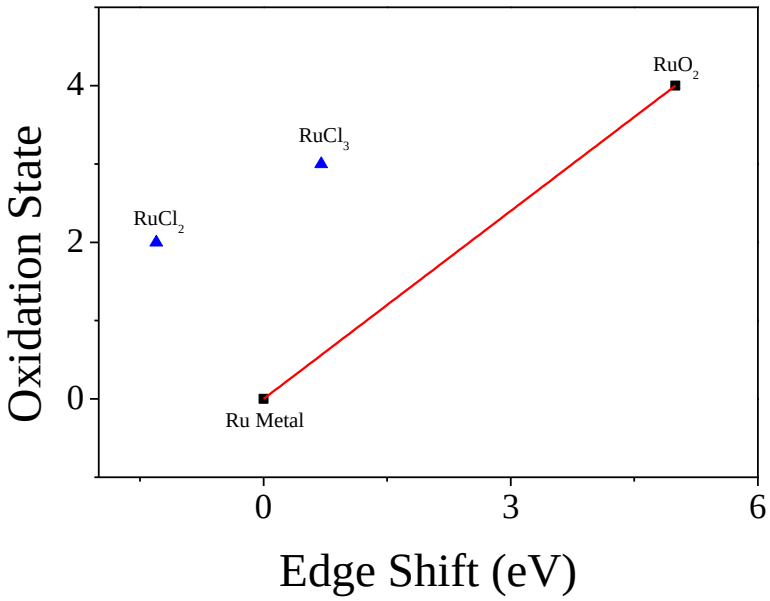

Figure S7. Correlation of formal charge on Ru to edge shift for standards. Black standards indicate data points used for correlation. Blue standards were not used for correlation of experimental data.

Table S4. Gaussian results for percent density of HOMO and LUMO on each atom for $Ru(acac)_3$.

Atom	HOMO Density	LUMO Density
Ru	53.29%	66.55%
O	3.78%	2.74%
O	3.78%	2.74%
O	5.27%	3.12%
O	4.03%	3.51%
O	5.27%	3.12%
O	4.03%	3.51%
C	0.76%	0.67%
C	0.76%	0.67%
C	1.20%	1.26%
C	1.76%	1.62%
C	1.20%	1.26%
C	1.76%	1.62%
C	0.11%	0.07%
C	0.34%	1.95%
C	0.11%	0.07%
C	0.11%	0.16%
C	5.09%	1.64%
C	0.19%	0.21%
C	5.09%	1.64%
C	0.11%	0.16%
C	0.19%	0.21%
H	0.04%	0.02%
H	0.02%	0.02%
H	0.03%	0.02%
H	0.09%	0.22%
H	0.04%	0.02%
H	0.02%	0.02%
H	0.03%	0.02%
H	0.04%	0.06%
H	0.03%	0.03%
H	0.02%	0.08%
H	0.48%	0.20%
H	0.07%	0.10%
H	0.03%	0.02%
H	0.07%	0.08%
H	0.48%	0.20%
H	0.04%	0.06%
H	0.03%	0.03%
H	0.02%	0.08%
H	0.07%	0.10%
H	0.03%	0.02%
H	0.07%	0.08%